LARGE CRATERS ON THE METEOROID AND SPACE DEBRIS IMPACT EXPERIMENT

Donald H. Humes
NASA Langley Research Center
Hampton, VA 23665-5225
Phone: 804/864-1484, Fax: 804/864-7730

SUMMARY

Examination of 29.37 m² of thick aluminum plates from the Long Duration Exposure Facility, which were exposed to the meteoroid and man-made orbital debris environments for 5.8 years, revealed 606 craters that were 0.5 mm in diameter or larger. Most were nearly hemispherical. There was a large variation in the number density of craters around the three-axis gravity-gradient stabilized spacecraft. A new model of the near-Earth meteoroid environment, which uses a speed distribution proposed by Erickson and a direction distribution relative to the Earth, gives good agreement with the crater fluxes measured on the fourteen faces of the LDEF. The man-made orbital debris model of Kessler, which predicts that 16 percent of the craters would be caused by man-made debris, is plausible. No chemical analyses of impactor residue that will distinguish between meteoroids and man-made debris is yet available.

INTRODUCTION

For nearly six years, the Long Duration Exposure Facility (LDEF) orbited the Earth with 57 scientific experiments on board that were to be evaluated when the spacecraft was returned to the ground. There was no communication with the LDEF while it was in orbit. The Meteoroid and Space Debris Impact Experiment, designated S0001 by the LDEF Project Office, consisted of many thick aluminum plates distributed around the spacecraft to study the population, directionality, and chemical composition of meteoroids and man-made debris. All the data will be obtained from examination of the craters left in the aluminum plates.

In some places in the literature this experiment is referred to by a shortened title as the Space Debris Impact Experiment.

Meteoroids are small interplanetary particles that travel through our solar system undetected and whose encounter can only be treated statistically. They are natural particles that are in orbit about the sun. Meteoroids that pass near the Earth are drawn toward the Earth by its gravitational field and some strike spacecraft as they speed toward the atmosphere. Meteoroids have been considered a hazard to spacecraft since the beginning of space exploration. NASA has published models of the meteoroid environment near the Earth (ref.1) and in interplanetary space (ref.2), and a design criteria document for protection against meteoroids (ref.3). But the interest in meteoroids is broader than the concern about the hazard they present to spacecraft. Meteoroids may be unaltered primal material whose composition and orbital paths are important clues to the origin and evolution of the solar system.

Space debris is the man-made material left in space as a result of our space activity. It ranges in size from microscopic fragments created during explosions in space to large spent rocket motors. Some man-made debris escaped the Earth's gravity but most was left in orbit about the Earth. That space debris that is still in orbit about the Earth is of concern as a potential hazard to spacecraft. Large pieces of debris are tracked and cataloged and possible collisions with the Space Transportation System (STS) orbiter are checked for each mission so that evasive measures can be taken if necessary. Small pieces cannot be tracked and their encounter, like that of meteoroids, must be treated statistically. NASA now has a model of the man-made orbital debris environment (ref.4) to be used in hazard analysis.

The Meteoroid and Space Debris Impact Experiment is directed at both the hazard of impact damage and the nature of our solar system but this preliminary paper will deal primarily with the data most applicable to the hazard, i.e. the number and location of the large craters. All craters with diameters of 0.5 mm and greater (measured across the top of the raised lips) have been examined and their number density and distribution around the spacecraft is the primary topic of this report. The study of smaller craters is incomplete and they are referred to only briefly. No chemical analyses of the impacting particles is presented.

The LDEF maintained a three-axis gravity-gradient stable orientation, which provided a new level of sophistication in flight data on meteoroids and man-made debris. In previously obtained flight data in near-Earth space, see ref.1, the number of meteoroid impacts was obtained but the orientation of the impact site at the time of the impact was unknown. The number density of craters for the different fixed surface orientations provides a direct measurement of the degree to which the hazard to spacecraft is directional. The variation in the number density of craters with surface orientation depends on the orbital distribution of the particles. While the orbits of individual particles cannot be determined with this experiment, theoretical orbital distributions can be checked by seeing if they are in agreement with the crater distribution found on the LDEF.

Some aluminum plates donated to the LDEF Meteoroid and Debris Special Investigation Group (M&D SIG) by principal investigators of other LDEF experiments were examined and the results are included in this paper. Wayne Slemp donated the base plates, sample holders and cover plates from his experiment on the only side of the LDEF from which the Meteoroid and Space Debris Impact Experiment plates were missing. His contribution is especially significant because that side of the LDEF received the greatest concentration of impact craters. William Berrios donated a thermal panel from the space-facing end of the LDEF.

The dummy plates that covered two unused experiment compartments on the Earth-facing end of the LDEF were also examined and the results are included in this paper.

EXPERIMENTAL HARDWARE

The Meteoroid and Space Debris Impact Experiment exposed 26.32 m^2 of aluminum plate to the space environment. The plates were 4.8 mm thick and were made of aluminum alloy 6061-T6. They had a thin oxide layer on both sides produced by chromic anodization and a coat of black paint on the back for spacecraft thermal control.

The location of the Meteoroid and Space Debris Impact Experiment plates on the LDEF is shown in Fig.1 along with the location of the other hardware examined in this study. The plates were mounted on the bottom of the 7.6 cm deep trays, except for the plates in Tray D6, which were mounted even with the top of the tray.

The nineteen peripheral trays that were totally dedicated to this experiment had two plates measuring 0.62 m by 0.95 m in each tray. The three peripheral trays that were shared with other experiments had two plates measuring 0.41 m by 0.95 m in each tray. These individual plates are identified by the tray location number and the relative position of the two plates in the tray. For example, the two plates in the tray in location F10 are identified as plates F10G and F10H, with F10G being the plate nearest the G-end or Earth-facing end of the LDEF. The three end trays each contained a single plate that was 0.72 m by 0.72 m.

The plates donated by Wayne Slemp were from his B9 tray. They are anodized aluminum, 6061-T6, of various thicknesses from 1.6 mm to 6.4 mm and have an area of 0.62 m2 . The experiment was divided neatly into thirds in the tray (see Fig.2) and for the purposes of this report all the plates in the third nearest the Earth-facing end will be referred to as the B9G plates, those in the third nearest the space-facing end as the B9H plates, and those in the middle third as the B9M plates.

The thermal panel donated by William Berrios was anodized aluminum (6061-T6), 1.6 mm thick. It was attached to the space-facing end of the LDEF and had an edge that was bent to wrap around the corner of the spacecraft along the Row-6 side. Only the 0.63 m2 of the thermal panel that was on the space-facing end is included as a part of this report. This thermal panel is identified as 920-6F by the LDEF Project Office and as H19 by the LDEF M&D SIG.

The two dummy plates on the Earth-facing end were anodized aluminum (6061-T6), 2.3 mm thick. Each plate had an area of 0.90 m2. One was identified as G19-9 by the LDEF Project Office and as G9 by the LDEF M&D SIG, and the other as G21-3 by the LDEF Project Office and as G3 by the M&D SIG.

LDEF MISSION

The LDEF was deployed by the STS-41C crew on April 7, 1984. It was initially placed in a near-circular orbit with an apogee of 480 km, a perigee of 474 km, and an inclination of 28.5 degrees. By the time it was recovered by the STS-32 crew on January 12, 1990, it had fallen to an altitude of 331 km.

It was intended for the longitudinal axis of the spacecraft to be aligned with its Earth-centered position vector and for the normal to the Row 9 trays to be aligned with the velocity vector. Post-flight analysis showed that the actual orientation had a misalignment of about eight degrees in yaw and one degree in pitch, see ref.5. As a result, the leading edge of the LDEF was between Row 9 and Row 10. The one degree pitch angle gave the space-facing end a slight view of the forward direction of flight.

DESCRIPTION OF CRATERS

The craters in aluminum on the LDEF look very much like craters produced with hypervelocity accelerators in the laboratory at impact speeds greater than about 6 km/s. The craters are generally round with lips that rise above the surface of the plate. The photograph in Fig.3 shows the top view of a crater on the F10H plate. This 4 mm diameter crater is the largest on any of the Meteoroid and Space Debris Impact Experiment plates and is the largest crater examined in this study. A side view of another crater on the F10H plate is shown in Fig.4. The lips of this 2 mm diameter crater are touching, or nearly touching, the surface of the plate, which reflects their image at the extreme angle at which the photograph was taken.

Most of the craters are round and symmetric, which is surprising considering that the impacting particles were undoubtedly irregular in shape and must have struck at oblique angles. The dimensions of 27 large craters are given in Table I. Three measurements, the diameter at the top of the raised lips, the depth, and the diameter at the plate surface, were made. The diameter at the plate surface is considered to be a more fundamental dimension than the diameter at the top of the raised lips, but it is more difficult to measure and sometimes in the literature authors give only the lip diameter. Henceforth in this report "diameter" will refer to the diameter at the surface of the plate, which some refer to as the true diameter, and "lip diameter" will refer to the diameter at the top of the raised lips.

Nine of the craters in Table I were on the plates in the F3 tray. In general, the lowest impact speeds should occur on these plates because they are closest to the trailing edge of the spacecraft and the particles must catch up to the spacecraft to strike them. Nine of the craters were on the F10 plates. In general, very high speed impacts should occur on these plates because they are close to the leading edge of the spacecraft where head-on collisions occur. Despite the fact that the extreme differences in impact speed occur on the F3 and F10 plates, there is no noticeable difference in the shape of the craters. The other nine craters in Table I were on the H5 plate, which was on the space-facing end of the LDEF where impact speeds are intermediate. At all three locations, the diameter of the craters at the plate surface is about 0.75 times the diameter at the top of the raised lips. The depth of the craters is about 0.5 times the diameter at the plate surface, i.e. the craters are nearly hemispherical.

While the study of smaller craters, <0.5 mm lip diameter, on this LDEF experiment is not complete, many small craters on the F10H and H5 plates have been measured. Differences in the craters seem to be appearing at smaller sizes. Firstly, the small craters are not all round, i.e. they do not have a circular cross-section at the surface of the plate. About one percent of the craters measured to date on the F10H plate are oblong with the shortest axis being less than 0.7 times the longest axis. On the H5 plate, six to eight percent of the craters measured to date are that oblong. Secondly, the average depth-to-diameter ratio of the small round craters on the F10H plate is greater than that of the large craters, being about 0.55 for those craters measured to date that have lip diameters between 0.1 mm and 0.5 mm, and about 0.63 for those that have lip diameters less than 0.1 mm. The small round craters on the H5 plate have the same average depth-to-diameter ratio as the large craters on that plate.

There were no craters on any of the plates examined that penetrated through the entire thickness of the plate. The impact that created the largest crater on the Meteoroid and Space Debris Impact Experiment, the 4 mm crater on the F10H plate, produced a very short raised dome on the back of the 4.8 mm thick plate. The dome was less than 25 microns high. It is not known if it is just the black paint that delaminated and raised up or whether the aluminum plate is actually bulged. The two thinnest donated plates from Row 9 had a total of four craters in the 1.6 mm thick aluminum that caused the back of the plates to bulge. The 1.6 mm thick thermal panel from the space-facing end did not have any craters that produced a noticeable bulge on the back of the plate; however, the black paint on the back would make it more difficult to spot a bulge than on the unpainted plates from Row 9.

NUMBER AND LOCATION OF CRATERS

There were 532 craters on the Meteoroid and Space Debris Impact Experiment plates that had a lip diameter of 0.5 mm or greater. There were another 74 craters of that size on the other LDEF plates included in this study. The distribution of these 606 craters around the spacecraft is given in Table II. The orientation of the plates on the sides of the LDEF is given by the angle between the spacecraft velocity vector and the normal to the plate surface. The trays on each row are grouped together because the flux should be constant along a row for both meteoroids and man-made debris. The area of the plates is the actual area. No correction has been made for the shielding that occurs for the plates that were mounted on the bottom of the 7.6 cm deep trays.

The variation in crater flux with plate location is shown in Fig.5. The crater flux is the number density of craters divided by the duration of the mission. The flux is greatest near the front of the spacecraft and it decreases smoothly toward the back, except on the plates nearest the trailing edge where the flux increases again. The variation in the measured crater flux on the sides of the LDEF exceeds a factor of 20.

The error bars, which are the 90 percent confidence limits calculated using the chi-squared distribution function in the manner suggested in ref.6, are appreciable because of the small number of craters, especially near the back of the LDEF. It may be that the increase measured near the trailing edge is just a statistical variation. When the examination of these plates is complete, there probably will be more than 30,000 craters to consider and then, perhaps, it will be clear whether the increase in the flux near the trailing edge is real.

The data points in Fig.5 are alternately from the south-facing and the north-facing side of the spacecraft. The smoothness of the data shows that there is a north/south symmetry in the particulate environment in the size range considered in this report.

The flux on the space-facing end is about the same as it would be for a plate on the side of the LDEF that faces 60 degrees from the velocity vector and is about twice that for a plate on the side facing 90 degrees from the velocity vector.

The data points in Fig.5 are the average flux for each face. In most cases, all of the trays or plates on the same face give the same flux within the 90 percent confidence limits. The exception is the B9G and B9M groups of plates which were side-by-side but which differed by more than a factor of 3.3 in crater flux.

COMPARISON WITH CURRENT NASA MODELS

Meteoroids

The NASA model of the near-Earth meteoroid environment in ref.1 is a simple model that assumes that all meteoroids strike a spacecraft normal to the surface and at a speed of 20 km/s. A speed distribution for the meteoroids is given in ref.1, but the direction from which the meteoroids approach the spacecraft is not defined so that the model is used to calculate the average flux on a randomly tumbling spacecraft. It is not suitable for calculating the variation in flux around the LDEF. It could, of course, be used to calculate the number of craters that would be expected on a randomly tumbling LDEF.

The model gives the flux of meteoroids on a spacecraft as a function of mass although meteoroid mass was not measured directly in any of the experiments on which the model is based. Data from the Explorer 16, Explorer 23, and the Pegasus satellites, where the penetration rate for various detector thicknesses was obtained, provided much of the basis for the model. This data was converted to meteoroid mass using eq.1, an empirical equation that gives the thickness t, in cm, of a sheet of material that can be completely penetrated by a particle of mass m, in g, having a density ρ, in g/cm^3, when the impact speed is V_r, in km/s.

$$t = K_1\, m^{.352}\, \rho^{1/6}\, V_r^{.875} \tag{1}$$

The coefficient K_1 is a material constant equal to 0.54 for aluminum sheets. The model should provide excellent predictions of the penetration fluxes for thin sheets on randomly tumbling surfaces if the same

penetration equation originally used to convert the penetration data to meteoroid mass is used to convert meteoroid mass back to penetration capability. If a more accurate penetration equation is found and is used with the model, it will give the wrong meteoroid penetration flux.

However, the LDEF data presented in this report is not the number of penetrations through some thin sheet of material, but is instead, the number of craters above a given size in a thick plate. Therefore an equation is needed that gives the size of a crater produced by a meteoroid. The accuracy with which the model in ref.1 can predict the flux of craters above a given size depends on the relationship between this crater size equation and the penetration equation originally used to convert the flight data to meteoroid mass. The important thing is not whether the crater size equation is accurate but whether the ratio of crater size predicted to penetration thickness predicted by the original equation is correct. Of course, the goal is to obtain accuracy in both equations and in the meteoroid model. It must be remembered, however, that when a better equation for penetration thickness is obtained, the model will have to be revised correspondingly.

With only modest expectations then, the average flux of craters with a lip diameter of 0.5 mm or greater was calculated for a hypothetical randomly tumbling LDEF, using the near-Earth meteoroid environment model in ref.1 and the crater depth equation from ref.3, which for an aluminum plate is

$$P = 0.42 \; m^{.352} \; \rho^{1/6} \; V_r^{2/3} \tag{2}$$

where m is the particle mass, in g, ρ is the mass density of the particle, in g/cm^3, V_r is the speed, in km/s, and P is the crater depth from the surface of the plate, in cm. The depth of a crater having a lip diameter of 0.5 mm would be about 0.1875 mm (0.5 mm x 0.75 x 0.5), assuming the average crater shape seen in Table II. Using an average impact speed of 20 km/s and an average mass density for meteoroids of 0.5 g/cm^3, as suggested in ref.1, eq.2 gives a meteoroid mass of 7.0 x 10^{-7} g. The average flux of meteoroids of that mass and greater on a randomly tumbling spacecraft orbiting at an altitude of 477 km is, according to ref.1, 7.0 x 10^{-8} $m^{-2}s^{-1}$. For the 29.37 m^2 of aluminum plate considered in this study and the 1.82 x 10^8 s duration of the LDEF mission, that flux results in a predicted 374 meteoroid craters.

Man-made Orbital Debris

The man-made orbital debris model in ref.4 is more detailed than the meteoroid model in ref.1. It gives the velocity distribution of debris relative to a spacecraft, both speed distribution and direction distribution, and therefore predicts a crater flux that varies with location on the spacecraft.

This model gives the flux of man-made debris on a spacecraft as a function of particle diameter. The model is based on radar and optical measurements of orbiting objects where radar cross-section and optical intensity is measured and converted to particle size, and on penetration and crater size data from samples returned from the Solar Max spacecraft where penetration thickness and crater dimensions, for those impacts caused by man-made debris, were converted to particle diameter using empirical penetration equations and an assumed particle density. Man-made debris craters were identified by chemical analyses of impactor residue found in the craters.

This man-made orbital debris model assumes that the debris is in circular orbits and predicts that the LDEF, had it flown in its planned orientation, would not have been struck by man-made debris on the space-facing end, the Earth-facing end, or on the trailing edge. Because of the one degree forward pitch

angle, the space-facing end would be predicted to receive a small number of impacts. The flux of the man-made debris craters around the LDEF having diameters of 0.5 mm or greater, as predicted by the model in ref.4, is shown in Fig.6. Equation 3 was used to determine the mass of the debris required to make a 0.01875 cm deep crater. It is identical to eq.2 except that the effect of the impact angle is included.

$$P = 0.42 \; m^{.352} \; \rho^{1/6} \; V_r^{2/3} \; (\cos \theta)^{2/3} \tag{3}$$

The angle θ is the impact angle measured from the normal to the surface. It is stated in ref.3 that the crater depth depends on the impact angle, correlating with the normal component of velocity for impact angles within 60 degrees of the normal. While mentioned in the text in ref.3, this impact angle effect was not included in the equations presented. The use of the normal component of velocity to predict crater depth is common and may have been used to convert the Solar Max data to debris mass in the man-made orbital debris model.

If the man-made orbital debris model is accurate, man-made debris must have created about one-fourth of the large craters on the Row 6 plates, about 11 percent of those on the Row 9 plates, and much less than one percent of the craters on the Row 3 and Row 4 plates. The variation in the crater flux with the location on the spacecraft predicted by the man-made debris model is quite different from that found on the LDEF. This further suggests that meteoroids do indeed dominate the particulate environment in this size range. The model predicts 94 man-made debris craters with a lip diameter of 0.5 mm or greater on the LDEF surfaces being considered in this study, which is 16 percent of the number actually found on the LDEF.

Combined Models

The total number of meteoroid and man-made orbital debris craters predicted by the models is 468. The calculated number is lower than the actual number on the LDEF, perhaps because the oriented surfaces considered in this study do not approximate well a randomly tumbling plate of equal area, thus producing an error in the calculation of the meteoroid flux, or perhaps because the crater depth equation and the penetration thickness equation do not provide the proper relationship between the crater size a particle can produce and the thickness of material it can completely penetrate. It is clear, however, that a different type of meteoroid model is needed, one that gives the variation in flux with surface location or orientation.

NEW MODEL OF THE NEAR-EARTH METEOROID ENVIRONMENT

Approach

The deficiency in the current model of the near-Earth meteoroid environment (ref.1) is that the directionality of the meteoroids is not defined. The first approach taken in establishing a new model was to assume that meteoroids would approach a stationary spacecraft from all directions not shielded by the Earth with equal probability; i.e. the directionality of the meteoroids is random. There is some theoretical basis for such an assumption. Kessler showed in ref.7 that, averaged over the entire Earth, the distribution of the angles at which meteoroids enter the atmosphere is random, and Zook argues in ref.8 that for a long mission, the LDEF mission in particular, a spacecraft is in so many positions relative to the Earth, and the Earth is in so many positions relative to the sun that a large portion of space is viewed and that meteoroids appear to approach the position of the spacecraft with random directionality when all impacts over the duration of the mission are taken together.

In the very first model tested here, it was assumed that meteoroids would approach a stationary spacecraft randomly from all directions in the half-space above the spacecraft horizontal plane, i.e. the plane through the spacecraft position that is perpendicular to the zenith/nadir line. When spacecraft motion was taken into account, the model predicted well the flux on all fourteen faces of the LDEF.

However, when the model was expanded to include the regions of space below the horizontal plane that are not shielded by the Earth and its atmosphere, as it should be, agreement with the LDEF data was not quite as good. The flux predicted for the twelve sides of the LDEF was good but the flux predicted for the space-facing end was too low by more than 30 percent, which exceeds the 90 percent confidence limits for the data. It appears that the assumption of random directionality may not be completely accurate.

No attempt was made to understand theoretically the cause of the discrepancy. But, in order to provide a model of the near-Earth meteoroid environment that does not underestimate the meteoroid flux on a space-facing surface, directionality distributions that are skewed toward the zenith were tested, even though they have no basis in theory. The zenith distance, z, is the angle measured from the zenith to the direction from which a meteoroid would approach a stationary spacecraft. Values of the distribution constant C for a zenith distance distribution function f(z) of the form

$$f(z) = \sin(Cz) \qquad (4)$$

were tested to see if there was some value for which the model would accurately predict the fluxes on all fourteen faces of the LDEF. A value of 1.4 provided good agreement with the LDEF data. For a random distribution of meteoroid directions, C would have a value of one. When many more craters are included in the analysis, the random directionality will be re-examined, but for the time being, an artificial distribution of meteoroid directions is proposed for the new model of the near-Earth meteoroid environment.

The new model retains the essential elements of the previous model, i.e. the size distribution, mass density, and gravitational enhancement of the meteoroid flux near the Earth. The Earth shielding factor found in ref.1 and ref. 2 is not included as a separate factor because it is inherent in the directionality assumption.

The spatial density of meteoroids, i.e. the number of meteoroids per unit volume, is a concept introduced in the interplanetary meteoroid environment model in ref.2 that is also used in this model. Spatial density can be inferred in ref.1 from the flux and average velocity, but it was not developed there as a property of the meteoroid environment.

The crater depth equation from ref.3, with the effect of impact angle included (eq.3), is accepted here and thus becomes an integral part of this new near-Earth meteoroid environment model.

Different meteoroid speed distributions, direction distributions, and spatial densities were examined and the combination that gave the best agreement with the crater flux found on the various faces of the LDEF was selected.

It is assumed that the size distribution, speed distribution and the direction distributions of the meteoroids are all independent of each other.

Some details of the proposed new model of the near-Earth meteoroid environment are given in the following five sections.

Directionality

The probability density for meteoroids approaching a spacecraft position with a zenith distance, z, is taken to be

$$f(z) = \sin(1.4\,z) \Big/ \int_{0°}^{128.6°} \sin(1.4\,z)\,dz \qquad 0° \leq z < 128.6° \qquad (5)$$

$$f(z) = 0 \qquad\qquad 128.6° \leq z \leq 180° \qquad (6)$$

The probability of meteoroids approaching a spacecraft from within 51.4 degrees of the spacecraft/Earth line becomes zero. Thus the Earth shielding is effectively constant for all altitudes above 2000 km. For spacecraft below an altitude of 2000 km, the shielding from meteoroids provided by the Earth and its atmosphere, assumed to be 165 km high, varies with altitude.

Two angles define the meteoroid directionality, the zenith distance is one, the azimuth is the other. The azimuth is the angle from a reference direction in the horizontal plane of the spacecraft. The probability density for meteoroids approaching a spacecraft with an azimuth, a, is independent of a and is

$$f(a) = 1/360 \qquad\qquad 0° \leq a \leq 360° \qquad (7)$$

Speed Distribution

The speed distribution of meteoroids, as given in refs.1,9,10 and 11, is the speed distribution of meteors observed in the Earth's atmosphere corrected to a constant meteoroid mass. It gives the fraction of the meteoroid flux on the atmosphere that is in various speed ranges. There is a bias in the observational data of meteors toward the faster meteoroids because they produce more easily detected radar and optical trails. As a result, smaller and more numerous meteoroids are observed at the higher velocities. The differences in the speed distributions from refs.1,9,10 and 11 are caused largely by the methods used to extract this bias from the data and get the speed distribution for constant mass meteoroids.

Because the concept of spatial density is being used in this new model, the speed distribution of meteoroids in a volume of space is required, and that is different from the speed distribution of the meteoroid flux on the atmosphere. For a unidirectional flow of particles, the relationship between the spatial density, S, and the flux, ϕ, on a surface perpendicular to the flow direction is

$$\phi = S\,V \qquad\qquad (8)$$

where V is the speed. Thus the speed distribution of meteoroids striking the atmosphere can be

transformed to the speed distribution of meteoroids in a volume of space just outside the atmosphere with the relationship

$$f(V) = (f_\phi(V)/V)/ \int_V f_\phi(V)/V \ dV \qquad (9)$$

where $f(V)$ is the probability density for meteoroids in a volume of space having speed V, and $f_\phi(V)$ is the probability density for meteoroids striking the atmosphere with speed V.

The speed distributions from refs.1,9,10,and 11 were tested in the new model. The speed distribution from ref.1 has more high speed meteoroids than the others and does not give enough variation in crater flux around the LDEF, while the speed distribution in ref.9 has an abundance of very low speed meteoroids and gives too great a variation in crater flux. The speed distributions found to provide the best agreement with the crater distribution found on the LDEF are those proposed by Erickson (ref.10) and by Kessler (ref.11). These independently derived distributions, which used different sets of meteor data, are nearly identical. A mathematical description of the Erickson speed distribution is given by Zook in ref.12 as

$$f_\phi(V) = 0.112 \qquad\qquad 11.1 \le V < 16.3 \text{ km/s} \qquad (10)$$

$$f_\phi(V) = 3.328 \times 10^5 \ V^{-5.34} \qquad 16.3 \le V < 55 \text{ km/s} \qquad (11)$$

$$f_\phi(V) = 1.695 \times 10^{-4} \qquad\qquad 55 \le V \le 72.2 \text{ km/s} \qquad (12)$$

where $f_\phi(V)$ is the probability density for meteoroids entering the atmosphere with speed V, in km/s. These equations also describe the Kessler speed distribution.

Density

The mass density of 0.5 g/cm^3 for meteoroids, given in both ref.1 and ref.2, is adopted for the new model.

Gravitational Focusing

The flux of meteoroids on a spacecraft is enhanced by gravitational focusing, so that the closer the spacecraft is to the Earth, the greater the meteoroid flux tends to be. In this new model, as in ref.2, the flux on a spacecraft is calculated, firstly, ignoring gravitational focusing, and then, that flux is multiplied by the gravitational enhancement factor, G, which from ref.2 is

$$G = 1 + 0.76 \ (r_e/r) \qquad (13)$$

where r_e is the radius of the Earth and r is the distance of the spacecraft from the center of the Earth.

408

Spatial Density and Size Distribution

The spatial density of meteoroids used in the new model is 2.33 times the spatial density given in ref.2 at 1 AU, thus preserving the size distribution of meteoroids inherent in the spatial density function. The spatial density, S, in no./m³, is therefore taken to be

$$\log_{10} S = -17.775 - 1.584 \log_{10} m - 0.063 (\log_{10} m)^2 \qquad m \leq 10^{-6} \text{ g} \qquad (14)$$

$$\log_{10} S = -17.806 - 1.213 \log_{10} m \qquad m > 10^{-6} \text{ g} \qquad (15)$$

where m is the meteoroid mass, in g.

Using the Model to Calculate Crater Flux

Meteoroids that approach a spacecraft from some small region of space, with speeds in the small speed range around V, will produce a crater in an aluminum plate that is deeper than P, if their mass exceeds m, where

$$m = P^{2.84} / ((0.42)^{2.84} \rho^{.473} V_r^{1.894} (\cos \theta)^{1.894}) \qquad (16)$$

and where V_r is the relative speed between the spacecraft and the meteoroid and θ is the impact angle on the plate relative to the normal to the plate surface. This is eq.3 with the terms rearranged. The spatial density of meteoroids of mass m and greater is obtained from eq.14 or eq.15. The flux of meteoroids of mass m and greater on the plate, and hence the flux of craters of depth P and deeper, from this small component of the meteoroid environment is

$$\Delta \phi = G S V_r \cos \theta f(z) \Delta z \, f(a) \Delta a \, f(V) \Delta V \qquad (17)$$

where Δz is the size of the zenith distance range and Δa is the size of the azimuth range of the region of space being considered, and ΔV is the size of the speed range being considered. The meteoroid velocity relative to the spacecraft, and relative to the Earth, both appear in this equation.

The total flux of craters from the entire meteoroid environment is obtained by summing the contributions to the flux from all speed ranges and from all regions of space not shielded by the Earth. Care must be taken to make sure that the proper units are used in eq.17 where V has been expressed in km/s and S in m⁻³, and one must be converted to make the length units consistent.

Comparison with the LDEF Data

The crater flux predicted by the new near-Earth meteoroid environment model of this paper for the fourteen faces of the LDEF is shown in Fig.7. The agreement with the data is excellent with the exception of the face nearest the trailing edge. The disagreement for the Earth-facing end is not significant because the measured flux is based on only one crater.

While the LDEF provides the best data on meteoroid impacts on an orbiting spacecraft, some consideration should be given to the flight data used to form the original near-Earth meteoroid environment model in ref.1, particularly the data from the 406-micron-thick aluminum penetration detectors on the Pegasus satellite. The penetration flux for that detector was 5.6×10^{-8} penetrations/m^{2}s (ref.13). The value of 8.0×10^{-8} m^{-2}s^{-1} that appears in ref.1 is a hypothetical flux derived from the Pegasus data for the case of an Earth with a gravitational field but no size to shield the spacecraft from meteoroids.

The accuracy with which the new near-Earth meteoroid environment model will predict the Pegasus penetration flux depends on the relationship between the penetration thickness equation selected and the crater depth equation that is an integral part of the new model. The equation used in ref.1 to relate meteoroid properties to penetration thickness (eq.1) does not provide good agreement with the Pegasus data when used with the new model, see Table III. It overestimates the penetration flux because it uses the impact velocity instead of the normal component of the impact velocity. Modifying eq.1 to include the effect of impact angle, improves the agreement somewhat but the penetration flux is still overestimated by a factor of 2.8, suggesting that the velocity dependence may be wrong.

A new penetration thickness equation is proposed where the velocity dependence for complete penetration is assumed to be the same as that for crater formation at meteoroid impact speeds. It is

$$t = K \, m^{.352} \, \rho^{1/6} \, V_r^{2/3} \, (\cos \theta)^{2/3} \qquad (18)$$

where K is a material constant that was determined to be 0.72 for aluminum by requiring that two conditions be satisfied. Firstly, eq.18 must predict about the same penetration thickness as eq.1 in the 5 km/s to 8 km/s speed range because eq.1 is an empirical equation derived from laboratory tests in that speed range. It agrees within 14 percent. Secondly, when eq.18 is used in the new near-Earth meteoroid environment model, the predicted flux for the Pegasus detector must be about the same as the measured flux. It agrees within 17 percent.

DISCUSSION

The new model of the near-Earth meteoroid environment predicts crater fluxes of 0.5 mm diameter and greater craters on the fourteen faces of the LDEF that are in good agreement with the measured fluxes, for the most part. The exception, for the face nearest the trailing edge, is taken to be the result of a statistical variation in the measured flux.

The new meteoroid model accounts for all the craters found on the LDEF plates studied. No adjustment has been made to make the combined meteoroid and man-made debris models predict precisely the total number of craters found on the LDEF because the accuracy of the models is not expected to be near 16 percent, i.e. the contribution from man-made debris to the total flux.

The directionality proposed for the meteoroids, specifically the zenith distance dependence, gives a greater flux on the space-facing end of the LDEF relative to the sides than a random distribution of meteoroid directions would give. When random directionality is used in this new model and the spatial density is adjusted so that 606 craters are predicted, the crater flux on the space-facing end is only 1.4×10^{-7} m^{-2}s^{-1}, compared to the measured flux of 2.0×10^{-7} m^{-2}s^{-1}. When the zenith distance probability density function given in this paper is used, the predicted crater flux on the space-facing end is 1.9×10^{-7} m^{-2}s^{-1}.

The fraction of the craters that were caused by man-made debris is not known. Hopefully, impacting particle residue will be found in the craters and chemical analyses will distinguish between meteoroids and man-made debris. Because the model of the man-made debris environment predicts that the debris would create only 16 percent of the craters found on the LDEF, it is entirely plausible.

REFERENCES

1. Meteoroid Environment Model - 1969 (Near Earth to Lunar Surface). NASA Space Vehicle Design Criteria (Environment). NASA SP-8013, 1969.

2. Meteoroid Environment Model - 1970 (Interplanetary and Planetary). NASA Space Vehicle Design Criteria (Environment). NASA SP-8038, 1970.

3. Meteoroid Damage Assessment. NASA Space Vehicle Design Criteria (Structures). NASA SP-8042, 1970.

4. Kessler, D.J.; Reynolds, R.C.; and Anz-Meador, P.D.: Orbital Debris Environment for Spacecraft Designed to Operate in Low Earth Orbit. NASA Technical Memorandum 100471, 1989.

5. Peters, P. N.; Gregory, J. C.: Pinhole Cameras as Sensors for Atomic Oxygen in Orbit; Application to Attitude Determination of the LDEF. NASA CP-3134, 1992.

6. Alvarez, J.M.: Statistical Analysis of Meteoroid Penetration Data Including Effects of Cutoff. NASA TN D-5668, 1970.

7. Kessler, D.J.: A Guide to Using Meteoroid-Environment Models for Experiment and Spacecraft Design Applications. NASA TN D-6596, 1972.

8. Zook, H.A.: The Velocity Distribution and Angular Directionality of Meteoroids that Impact on an Earth-Orbiting Satellite. Lunar and Planetary Science Conference XVIII Abstracts, 1138-1139, 1987.

9. Southworth, R.B.; and Sekanina, Z.: Physical and Dynamical Studies of Meteors. NASA CR-2316, 1973.

10. Erickson, J.E.: Velocity Distribution of Sporadic Photographic Meteors. Journal of Geophysical Research, vol.7, no.12, 3721-3726, 1968.

11. Kessler, D.J.: Average Relative Velocity of Sporadic Meteoroids in Interplanetary Space. AIAA Journal, vol.7, no.12, 2337-2338, 1969.

12. Zook, H.A.: The State of Meteoritic Material on the Moon. Proceedings of the Sixth Lunar Science Conference, 1653-1672, 1975.

13. Naumann, R.J.: The Near-Earth Meteoroid Environment. NASA TN D-3717, 1966.

Table I. Dimensions of twenty-seven large craters on the Meteoroid and Space Debris Impact Experiment plates from LDEF.

Location	D_{lips}, mm	D, mm	P, mm	D/D_{lips}	P/D
F3	1.92	1.46	0.73	0.76	0.50
	1.50	1.16	0.58	0.77	0.50
	1.50	1.12	0.58	0.75	0.52
	0.97	0.72	0.37	0.74	0.51
	0.86	0.65	0.33	0.76	0.51
	0.75	0.56	0.33	0.75	0.59
	0.73	0.59	0.24	0.81	0.41
	0.64	0.45	0.24	0.70	0.53
	0.63	0.47	0.27	0.75	0.57
				0.75 ave	0.52 ave
F10	4.02	3.02	1.55	0.75	0.51
	2.04	1.58	0.75	0.77	0.47
	1.96	1.46	0.75	0.74	0.51
	1.44	1.09	0.59	0.76	0.54
	1.42	1.08	0.54	0.76	0.50
	1.34	1.02	0.48	0.76	0.47
	1.22	1.06	0.52	0.87	0.49
	1.20	0.88	0.48	0.73	0.55
	1.14	0.82	0.41	0.72	0.50
				0.76 ave	0.50 ave
H5	1.12	0.89	0.41	0.79	0.46
	0.90	0.68	0.35	0.76	0.51
	0.85	0.63	0.32	0.74	0.51
	0.84	0.62	0.38	0.74	0.61
	0.75	0.57	0.29	0.76	0.51
	0.68	0.51	0.30	0.75	0.59
	0.68	0.55	0.25	0.81	0.45
	0.66	0.53	0.23	0.80	0.43
	0.62	0.50	0.23	0.81	0.46
				0.77 ave	0.50 ave

Table II. Location on LDEF of all large craters considered in this report.

Tray	Number	Area, m^2	Orientation, deg
B1	16	1.18	112
E1	20	1.18	112
F1	9	1.18	112
B2	5	1.18	142
D2	2	0.78	142
F3	9	1.18	172
C4	2	1.18	158
E4	7	1.18	158
A5	6	1.18	128
F5	7	1.18	128
A6	11	1.18	98
B6	16	1.18	98
D6	13	0.78	98
C7	32	1.18	68
E7	30	1.18	68
F7	39	1.18	68
B8G	17	0.39	38
B8H	21	0.39	38
B9G	29	0.227	8
B9M	7	0.185	8
B9H	15	0.207	8
F10G	46	0.59	22
F10H	32	0.59	22
B11	48	1.18	52
E11	50	1.18	52
F11	48	1.18	52
A12	26	1.18	82
H5	19	0.52	Space End
H19	23	0.63	Space End
G4	1	0.52	Earth End
G8	0	0.52	Earth End
G19-9	0	0.90	Earth End
G21-3	0	0.90	Earth End

Note: Orientation for trays on the sides of the LDEF is the angle between the normal to the tray surface and the spacecraft velocity vector.

Table III. Calculated penetration flux for 406-micron-thick aluminum detectors on the Pegasus satellites using the new near-earth meteoroid environment model and various penetration equations.

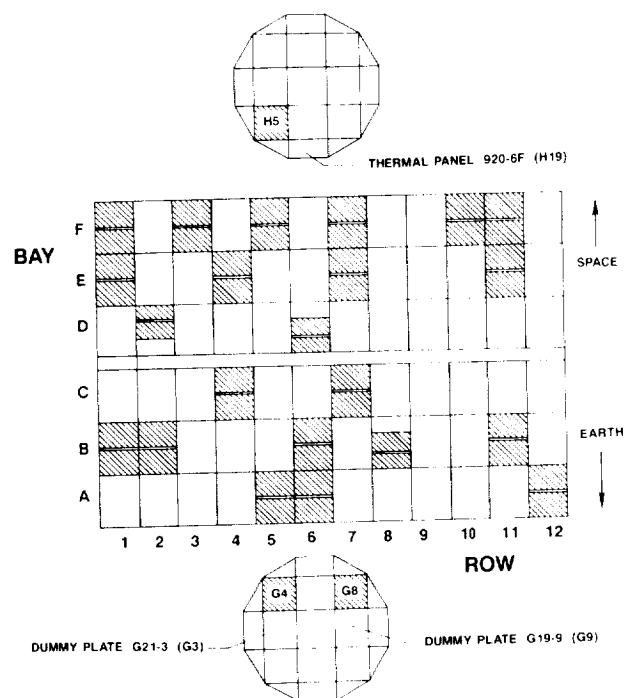| Penetration Equation	Source	Calculated Penetration Flux, $m^{-2}s^{-1}$
$t = 0.54 \ m^{0.352} \ \rho^{1/6} \ v^{0.875}$	ref. 1	3.29×10^{-7}
$t = 0.54 \ m^{0.352} \ \rho^{1/6} \ v^{0.875} \ (\cos \theta)^{0.875}$	ref. 1 (modified)	1.56×10^{-7}
$t = 0.72 \ m^{0.352} \ \rho^{1/6} \ v^{2/3} \ (\cos \theta)^{2/3}$	this paper	6.55×10^{-8}

414

Fig. 1. Identification system used for the tray locations on the LDEF. The shaded areas show the location of the Meteoroid and Space Debris Impact Experiment plates. The location of the thermal panel and dummy plates used in this study are also shown.
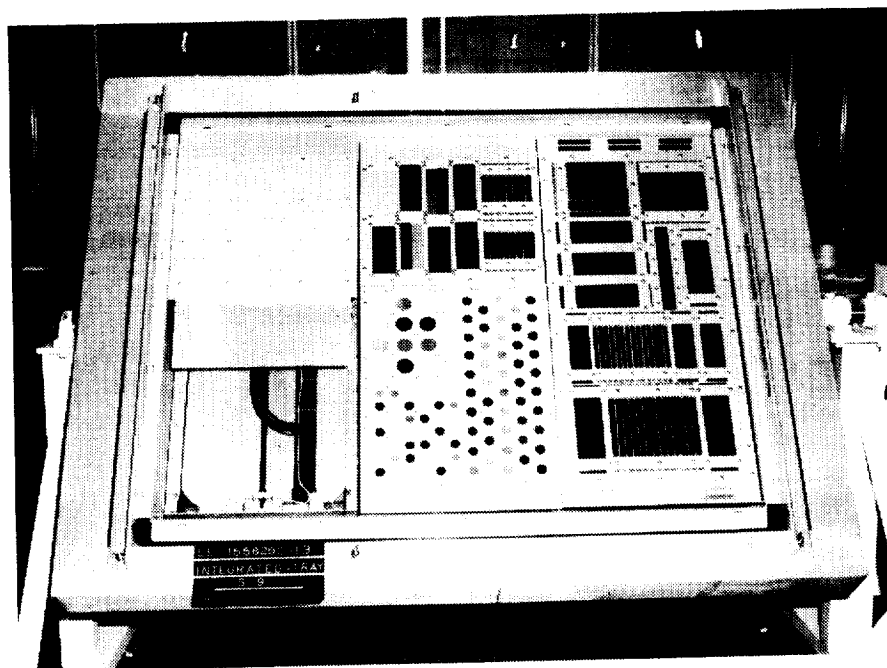

Fig. 2. Tray B9 containing aluminum plates donated by Wayne Slemp to the LDEF M&D SIG that were examined and included in this study.
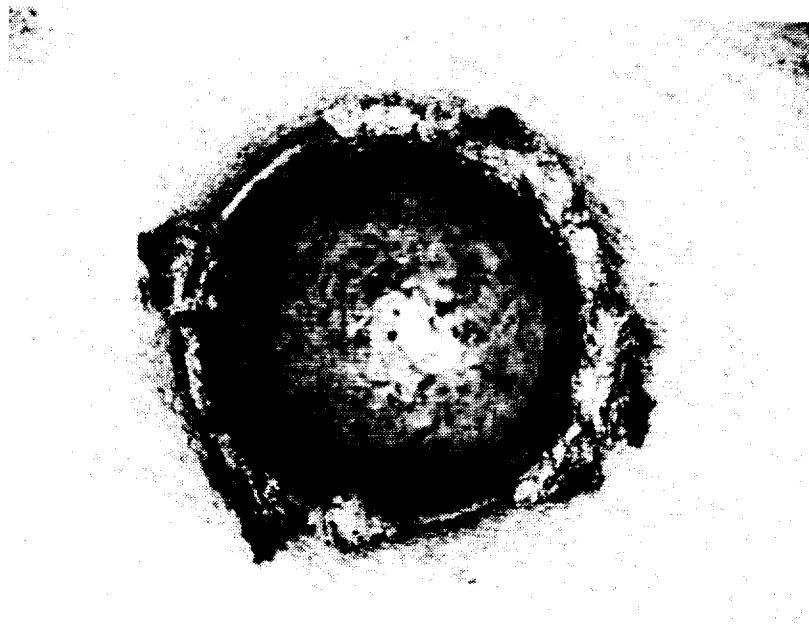
Fig. 3. Largest crater on the Meteoroid and Space Debris Impact Experiment. A 4 mm diameter crater on plate F10H.

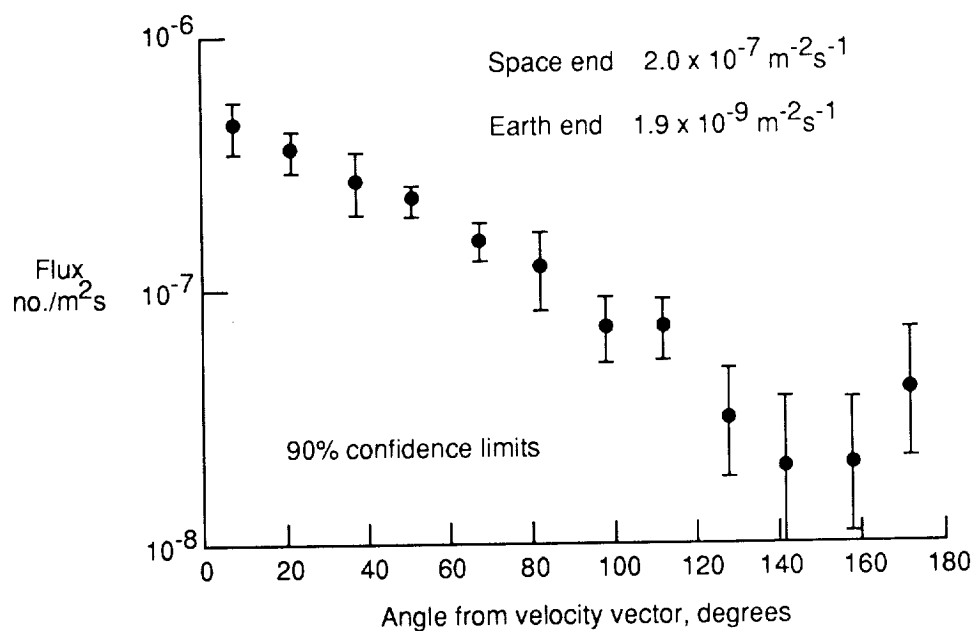Fig. 4. Side view of a 2 mm diameter crater on plate F10H.

416

Fig. 5. Measured crater flux around the LDEF for craters with a lip diameter of 0.5 mm or greater.
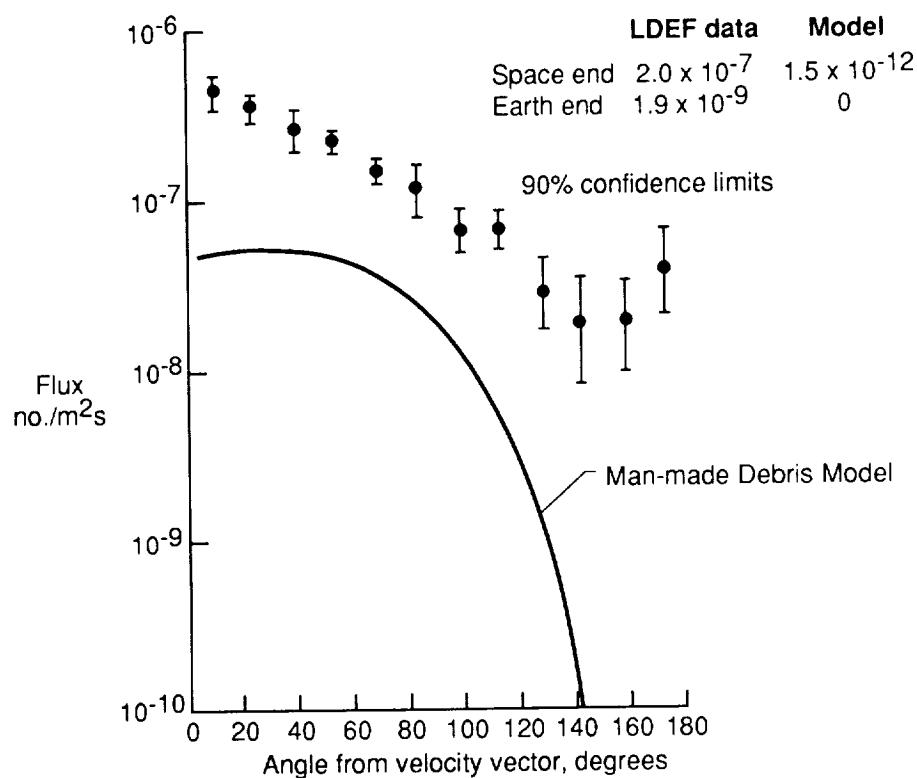

Fig. 6. Predicted crater flux from man-made orbital debris using the model in ref. 4 by Kessler, for craters with a lip diameter of 0.5 mm or greater.
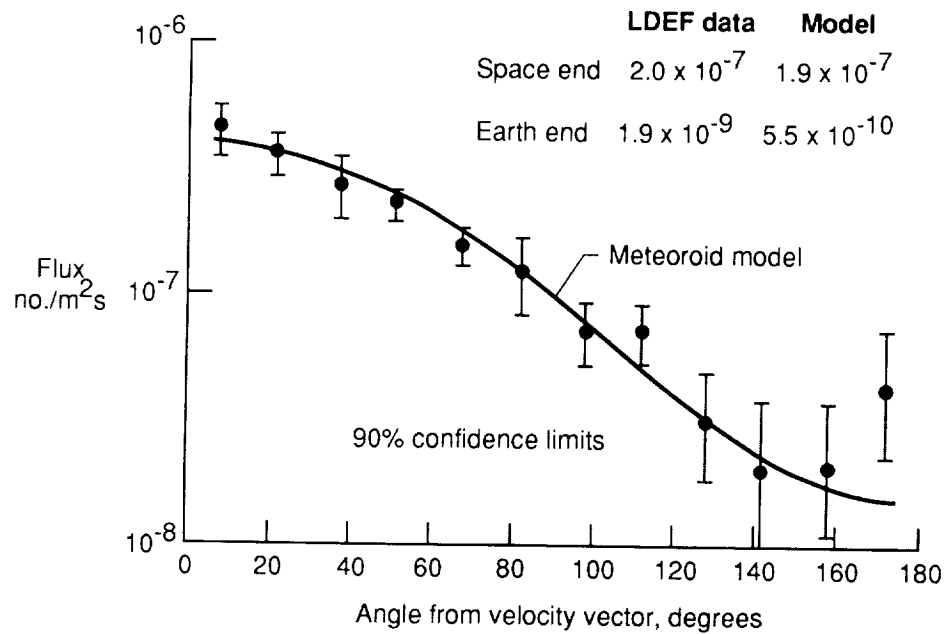
Fig. 7. Predicted crater flux from meteoroids using the new near-Earth meteoroid environment model proposed in this paper, for craters with a lip diameter of 0.5 mm or greater.